Surname *et al. Energy Mater* Year;Volume:Number
DOI: 10.20517/energymater.2021.xx

Energy Materials

Supplementary Material:

In-situ Li_2O-atmosphere assisted solvent-free route to produce highly conductive $Li_7La_3Zr_2O_{12}$ solid electrolyte

Jiawen Tang[1], Yongjian Zhou[1], Xiaoyi Li[1], Xiao Huang[1]*, Wei Tang[2], Bingbing Tian[1]*

[1]International Collaborative Laboratory of 2D Materials for Optoelectronics Science and Technology of Ministry of Education, Institute of Microscale Optoelectronics, Shenzhen University, Shenzhen 518060, Guangdong, China.

[2]Shaanxi Key Laboratory of Energy Chemical Process Intensification, School of Chemical Engineering and Technology, Xi'an Jiaotong University, Xi'an, Shaanxi 710049, China

***Correspondence to:** Dr. Xiao Huang, Institute of Microscale Optoelectronics, Shenzhen University, 3688 Nanhai Road, Nanshan District, Shenzhen 518060, Guangdong, China. E-mail: xiao199198@gmail.com; Prof Bingbing Tian, Institute of Microscale Optoelectronics, Shenzhen University, 3688 Nanhai Road, Nanshan District, Shenzhen 518060, Guangdong, China. E-mail: tianbb2011@szu.edu.cn

Table 1. Abbreviations with corresponding full name in the text.

Full Name	Abbreviation
relative density	RD
abnormal grain growth	AGG
terminal frequency	TF
distribution of relaxation times	DRT
standard deviation	S.D.
isopropanol	IPA
liquid electrolyte	LE
$Li_6Zr_2O_7$	LiZO
$Li_{6.55}La_3Zr_{1.55}Nb_{0.45}O_{12}$(0% excessive Li)	Nb4.5Li0
$Li_{6.55}La_3Zr_{1.55}Nb_{0.45}O_{12}$(0% excessive Li)+0/2/4wt% $Li_6Zr_2O_7$ (Li0L0/2/4) additive	Li0L0/Li0L2/Li0L4 or Nb4.5Li0L0/Nb4.5Li0L2/Nb4.5Li0L4

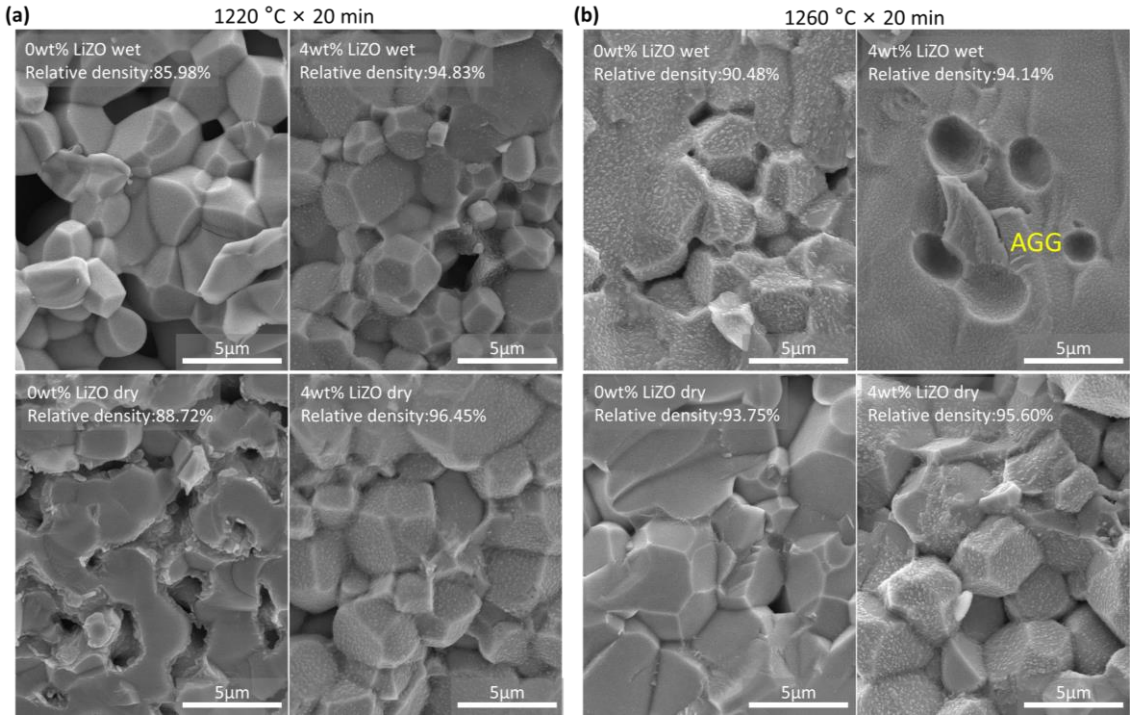

Figure 1. Cross-section SEM images of the Li0L0 and Li0L4 pellets sintered at (a) 1220 °C × 20 min and (b) 1260 °C × 20 min.

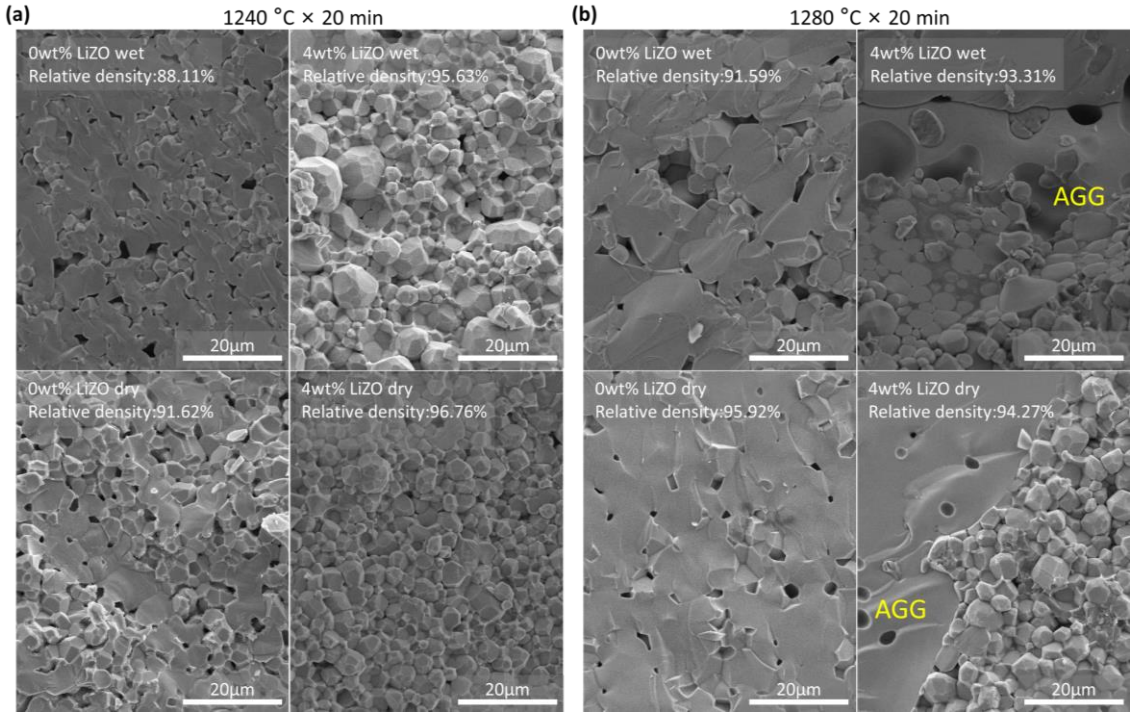

Figure 2. Cross-section SEM images of the Li0L0 and Li0L4 pellets sintered at (**a**) 1240 °C × 20 min and (**b**) 1280 °C × 20 min.

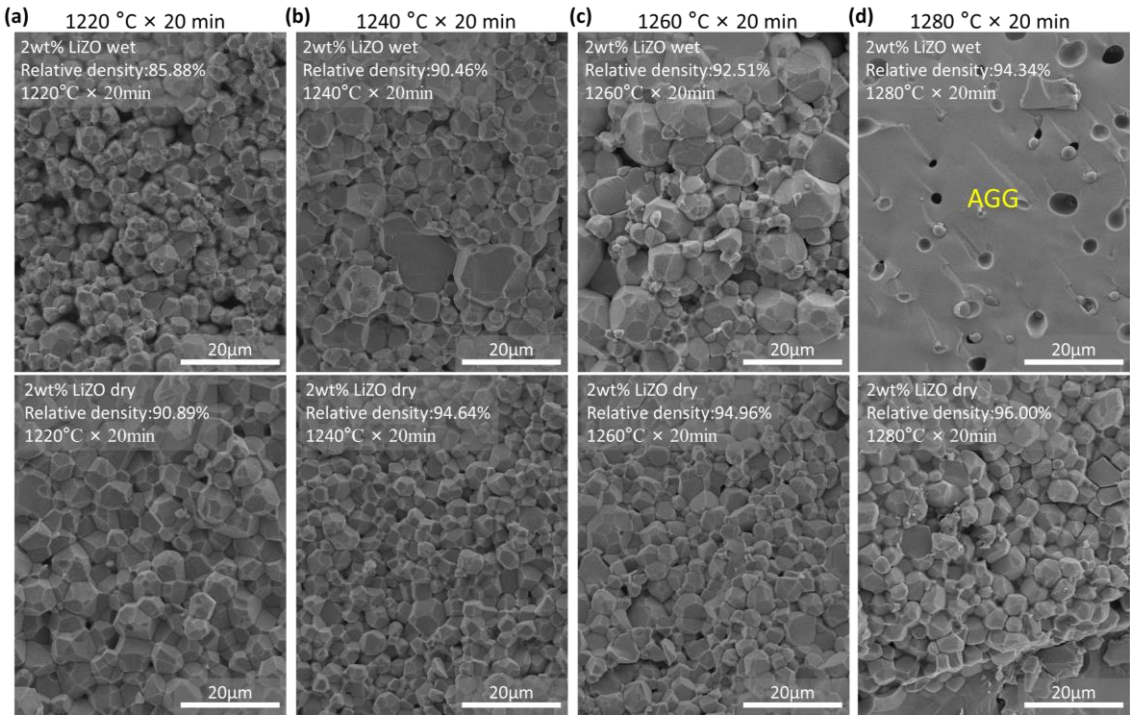

Figure 3. Cross-section SEM images of the Li0L2 pellets sintered at (**a**) 1220 °C × 20 min, (**b**) 1240 °C × 20 min, (**c**) 1260 °C × 20 min, and (**d**) 1280 °C × 20 min.

Surname *et al. Energy Mater* Year;Volume:Number | http://dx.doi.org/10.20517/energymater.2021.xx

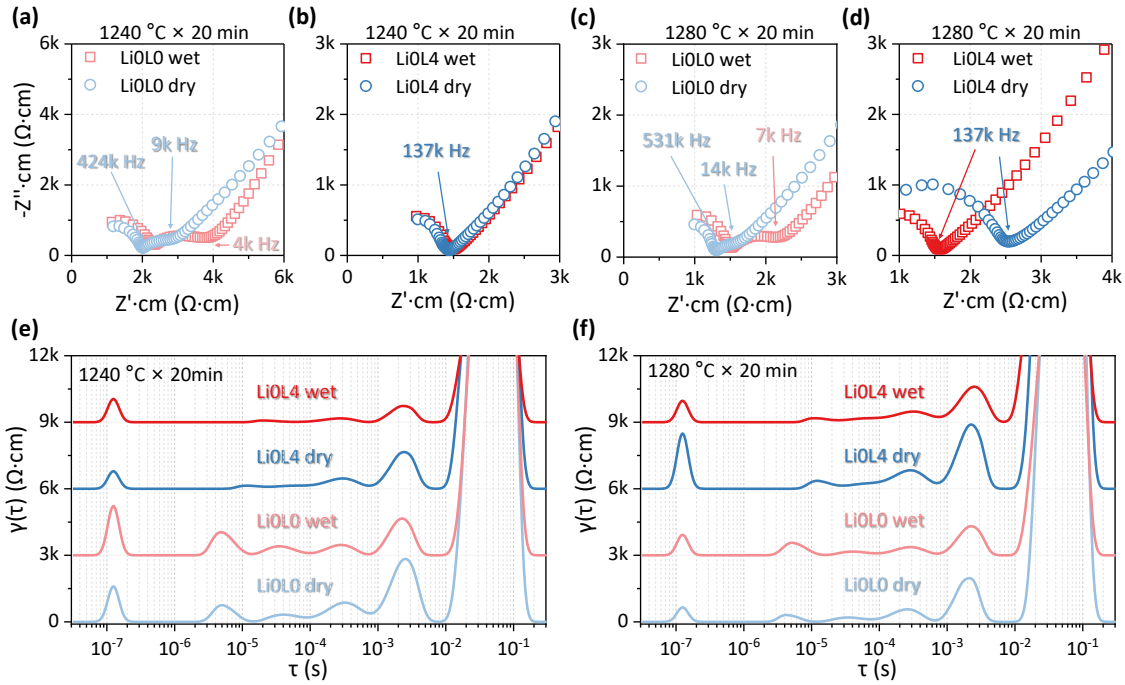

Figure 4. Electro-chemical properties of ceramics. Normalized Nyquist plots of (a) Li0L0 and (b) Li0L4 ceramics sintered at 1240 °C × 20 min; (c) Li0L0 and (d) Li0L4 ceramics sintered at 1280 °C × 20 min; (e and f) DRT transition of Nyquist plots in (a-d).

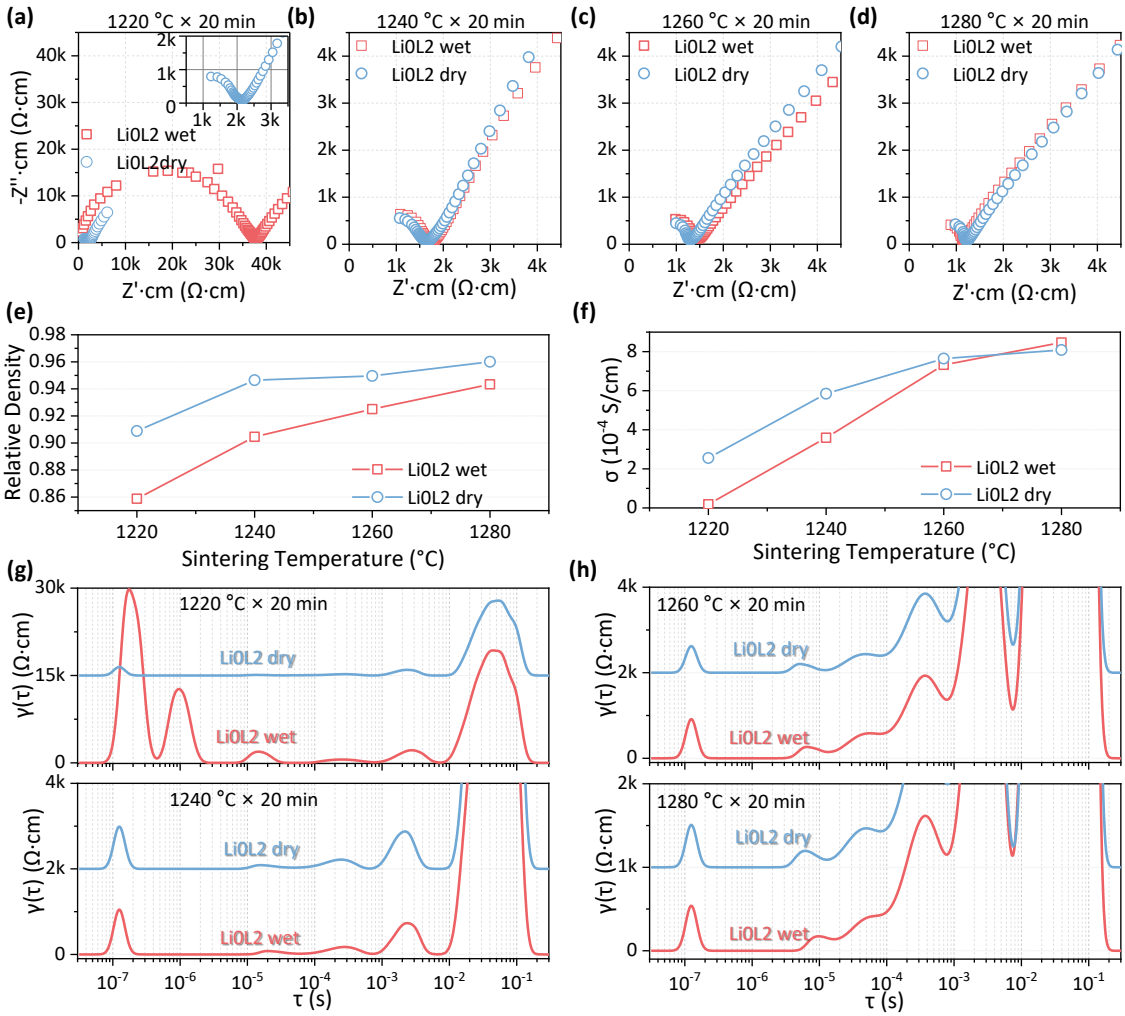

Figure 5. Electro-chemical properties and relative density of ceramics. Normalized Nyquist plots of Li0L0 sintered at (a) 1220 °C × 20 min, (b) 1240 °C × 20 min, (c) 1260 °C × 20 min and (d) 1280 °C × 20 min; (e) Relative densities and (f) Li^+ conductivities of Li0L2 sintered at 1220 °C ~ 1280 °C for 20min; (g and h) DRT transitions of Nyquist plots in (a-d).

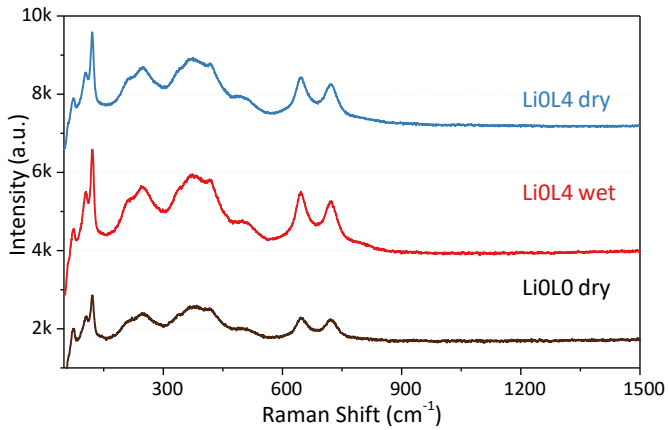

Figure 6. Second phase species analysis at grain boundary. Cross-section Raman spectra of Li0L0 dry, Li0L4 wet, and Li0L4 dry pellets.

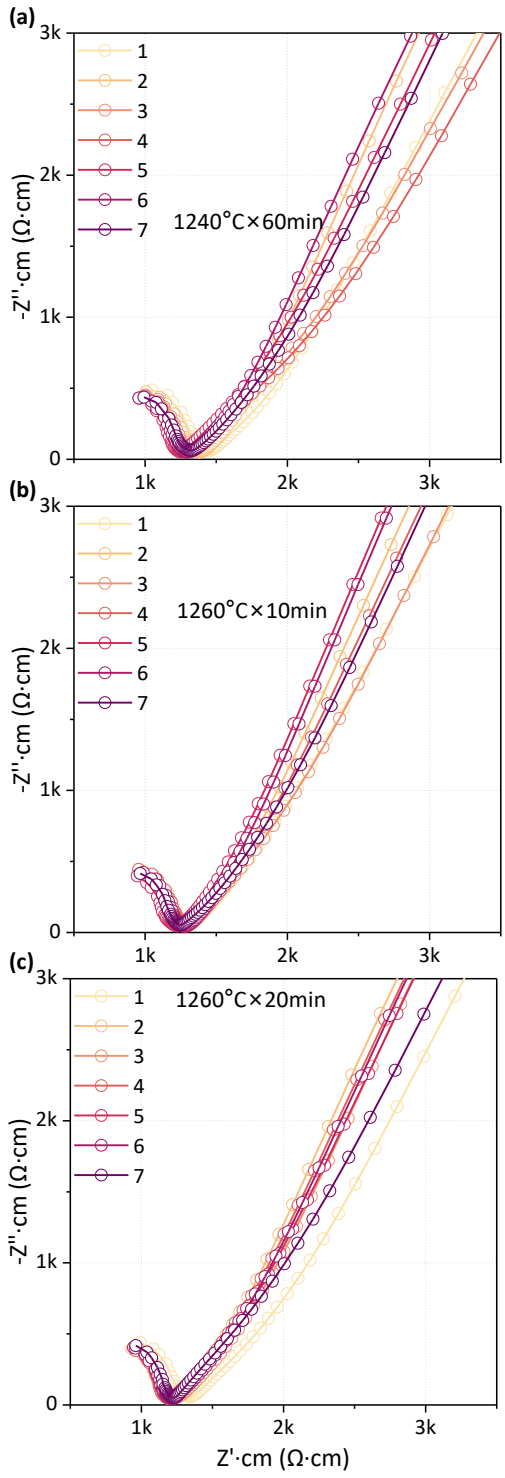

Figure 7. Inspection concerning consistency of mass-produced ceramics. Consistency in normalized Nyquist plots of Li0L2 dry sintered at (a) 1240 °C × 60 min, (b) 1260 °C × 10 min, and (c) 1260 °C × 20 min.

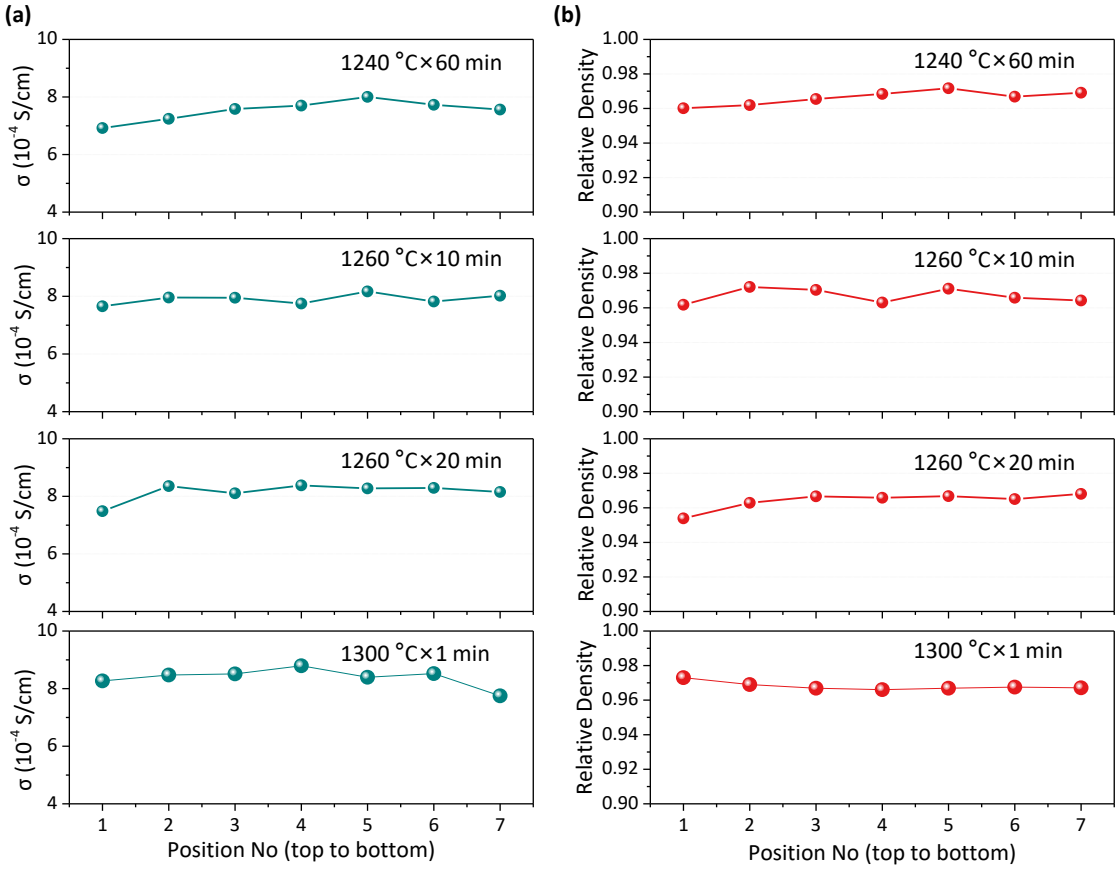

Figure 8. Inspection concerning consistency of mass-produced ceramics. Parallel information of (a) Li^+ conductivities, and (b) relative densities.

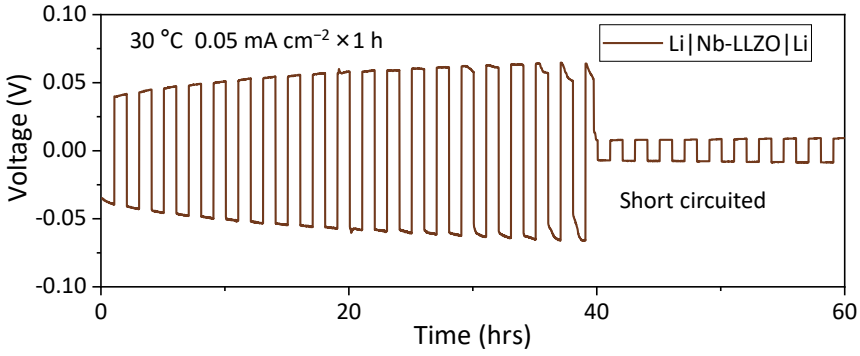

Figure 9. Galvanostatic cycling performance of Li-Li symmetric battery fabricated with scalable prepared Li0L2-dry pellets sintered at 1300 °C for 1 min without LE.

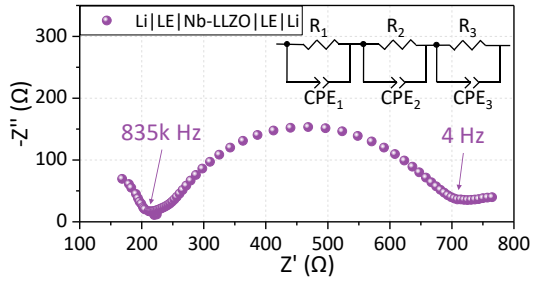

Figure 10. Nyquist plots of Li-Li symmetric battery. The first semicircle in frequency range of 8 MHz

to 835 kHz was assigned to the LLZO ceramic containing bulk and grain boundaries. The second semicircle from 835 kHz to 4 Hz corresponded to the interfacial charge transfer impedance ($Li^+ + e^-$ ↔ Li) between LLZO and the reversible Li electrode. The third flattened tail was attributed to the polarization of the symmetric cell at low frequencies, where the Li stripping and plating occurred on a time scale of 0.005~1 s.

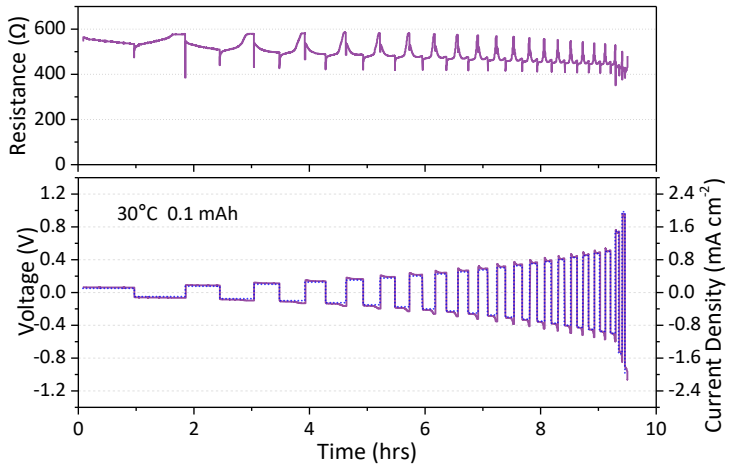

Figure 11. Rate performance using the capacity-constant mode of Li-Li symmetric battery.

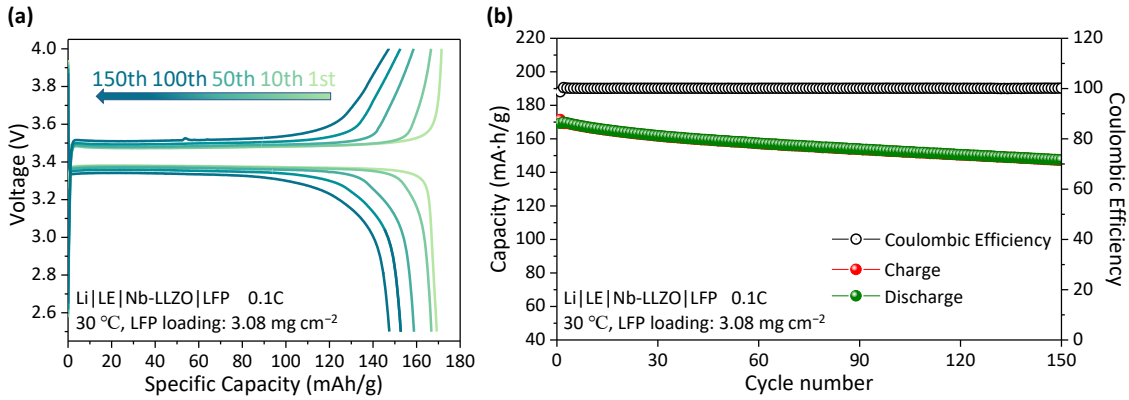

Figure 12. (a) Voltage profiles and (b) galvanostatic cycling performance of Li-LFP battery at 0.1C.